



7-1-1

**ON DYNAMIC INSTABILITY OF STRUCTURES
SUBJECT TO DYNAMIC EXCITATION
— A TRIAL REGARDING PREDICTION OF INCIPIENT INSTABILITY —**

Haruo KUNIEDA¹

1. Disaster Prevention Research Institute, Kyoto University
Uji, Kyoto 611, JAPAN

SUMMARY

Critical excitation of a single-degree-of-freedom system is discussed, which has a nonlinearity of quadratic as well as cubic terms of dependent variable. First, critical intensities of three type excitation are obtained by numerical calculation and their dependent property on system parameters is clarified. Then, possibility of analytic prediction of critical excitation is examined, referring to numerical results. A few trials of prediction are executed for sinusoidal excitation and several properties of respondent behaviour at stability limit are made clear, but this paper can not succeed yet to find the decisive method from a theoretical point of a view.

INTRODUCTION

Design criteria of space structures, vessels and some building structures subject to earthquakes depend often on whether respondent behaviours are hurtful for their functional safety or not, rather than on ultimate material strength of them. One of the most important respondent behaviours of the structures is concerned with dynamic instability as a whole of the structure.

Dynamic instability phenomena of the system with nonlinear restoring character have been investigated as Chaos problem in recent decade in the world(Ref.1). Respondent behaviours, i.e. chaotic behaviours, manifest themselves through many numerical examinations. However, the effective method of prediction of incipient instability has not been obtained except some special cases(Ref.2). Whereas chaotic behaviours are discussed in infinite time region, dynamic instability of the structures under earthquake loading becomes significant in finite time, especially in short time, region. That is, the instability in transient region is important and for which influence of initial conditions seems not to be negligible. Though the stability critical intensity of step or impulsive loading can be easily determined(Ref.3), it is quite difficult to determine it in case of time dependent excitation because of system being nonconservative. Even for sinusoidal excitation there is no effective method of prediction of this critical amplitude except such a method as to observe the respondent behaviour calculated numerically in time history. This paper deals with some investigations regarding the prediction of incipient instability.

GOVERNING EQUATION

The responses of flexible structures under earthquake loading are significant

usually in fundamental mode or modes of sufficiently low degree. This implies that it is pertinent to introduce the assumption of flexural vibration. Introducing the mode superposition method, the final governing equation of the structure is deduced in the following form.

$$\theta_{0n} \ddot{T}_n + \theta_{1n} \dot{T}_n + \{ \theta_{2n} - \theta_{3n} Q(t) \} T_n + \sum_{s,r=1}^N \theta_{4n}(s,r) T_s T_r + \sum_{s,r,p=1}^N \theta_{5n}(s,r,p) T_s T_r T_p = \bar{P}(t) \{ \theta_{6n} + \sum_{s=1}^N \theta_{7n}(s) T_s \} \quad \dots (1)$$

or compactly
$$M \ddot{T} + K(T, \dot{T}, Q(T)) = P(T, t) \quad \dots \dots \dots (2)$$

Where $Q(t)$ and $\bar{P}(t)$ are longitudinal and lateral excitation, respectively. Coefficients $\theta_{0n} \sim \theta_{7n}$ are usually calculated easily as shown, for instance, in Ref.3 for spatial frames subject to combined vertical and horizontal earthquakes, in Ref.4 for spherical domes subject to vertical earthquakes.

Only primitive knowledge about nonlinear dynamics leads to the speculation that dynamic instability should be examined in multi-modal state in continuum mechanics. In this context, Ref.4 has shown that stability critical intensity of excitation in multi-modal state is less than that in single modal state, in spite of numerical results of limiting number of cases considered.

The state of $Q = 0$ will be more practical in flexible structures and for this state the most comprehensive procedure to predict dynamic instability will be formulated as follows. If P is a periodic function with period R , following relations seem to hold.

$$T(R) = T(0) = T_0, \quad \dot{T}(R) = \dot{T}(0) = \dot{T}_0 \quad \dots \dots (3)$$

Substituting another solution $T + Y$ into eq.(2) and linearizing the equation with respect to Y , we get

$$M \ddot{Y} + C(T) \dot{Y} + K(T) Y = 0 \quad \dots \dots (4)$$

If a mapping matrix A which satisfies the following equation is obtained,

$$A [Y(0), \dot{Y}(0)]^t = [Y(R), \dot{Y}(R)]^t$$

we can set a stability measure $\rho(A)$ as

$$\rho(A) = \max |\lambda_i|, \quad \lambda_i: \text{eigen value of } A$$

Stability of the origin $Y(t) = 0$, that is, stability of $T(t)$ is examined from the character of this measure. However, since coefficient term of Y can not be usually expressed in mathematically analytic form, eigen values of A are not calculated in analytic sense. And, moreover, satisfaction of eq.(3) has not been confirmed. Thence, this procedure is of no use for the problem discussed herein.

Though the importance to take account of the condition of coexistence of a few modes is evident, there is no practically effective method to determine critical excitation except the method in which critical excitation is discriminated by the observation of appearance of sudden increase of some absolute response measure calculated numerically in time history region.

DYNAMIC INSTABILITY IN SINGLE MODE

In order to examine the properties of dynamic instability single modal state represented in the following expression will be discussed in this paper.

$$\eta^2 \ddot{x} + \zeta \eta \dot{x} + x + \alpha x^2 + \beta x^3 = F(t) \quad \dots (5)$$

1. Numerical Results of Critical Excitation For Dynamic Instability

Intensity of critical excitation was determined by direct observation of respondent behaviour of $x(t)$ calculated numerically in time historical region.

Stability limit intensity of excitation depends on the time $t = t_1$ at which sudden increase of response initiates. Fluctuation of stability limit due to the variance of t_1 , however, is very small in transient region.

CASE 1: $F(t) = f_0 \sin t$. Stability critical amplitude f_{CR} is defined as f_0 for which $x(t)$ depicts such a path as shown in Fig.1. Some numerical results are given in Table 1 with following initial conditions

$$x_0 = 0.002, \dot{x}_0 = 0 \text{ and } x_0 = 0, \dot{x}_0 = f_0/(1-\eta^2) \text{ (if } \eta = 1, \dot{x}_0 = -f_0/2)$$

Influence of initial conditions and damping on f_{CR} is given in Table 2 and Table 3, respectively.

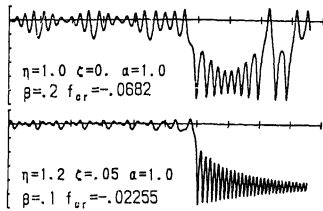


Fig.1 Examples of instability under sinusoidal excitation

Table 1 f_{CR} of sinusoidal excitation

α/β		$x_0=0.002, \dot{x}_0=0$			$x_0=0, \dot{x}_0=f_0/(1-\eta^2)$				
		0.10	-0.10	-0.30	-0.50	0.10	-0.10	-0.30	-0.50
$\eta = 0.8$	1.0	-0.07204	-0.06424	-0.05884	-0.05484	-0.09088	-0.08168	-0.07528	-0.07008
	0.5		-0.11364	-0.09124	-0.07864		-0.14496	-0.11696	-0.10096
	0.1		-0.15504	-0.11044	-0.09064		-0.19952	-0.14192	-0.11632
$\eta = 1.0$	1.0	-0.0535	-0.0460	-0.0400	-0.0345	-0.06056	-0.04136	-0.04168	-0.03440
	0.5		-0.0760	-0.0571	-0.0493		-0.08048	-0.07008	-0.05008
	0.1		-0.1014	-0.0700	-0.0590		-0.09776	-0.07856	-0.05936
$\eta = 1.2$	1.0	-0.15004	-0.11324	-0.10184	-0.10004	-0.20264	-0.18224	-0.16784	-0.15584
	0.5		-0.19624	-0.15904	-0.13884		-0.32272	-0.26512	-0.23312
	0.1		-0.26988	-0.19748	-0.19524		-0.44832	-0.33632	-0.28352
			-0.39548	-0.31548	-0.25748		-0.68616	-0.43792	-0.35032

(if $\eta = 1$, then $\dot{x}_0 = -f_0/2$.)

Table 2 Influence of x_0, \dot{x}_0 on f_{CR}

η	x_0	-0.042	-0.002	.038	.078	.118	.158	.198	.238	.278	.318	.358
0.8		-1136	-1136	-1128	-1111	-1085	-1051	-1009	-959	-902	-838	-769
1.0		-0753	-0751	-0812	-0816	-0758	-0733	-0753	-0762	-0810	-0817	-0721
1.2		-1928	-1959	-1990	-2023	-2055	-2051	-1984	-1913	-1838	-1762	-1681
	$\dot{x}_0 = 0$	$\alpha = 0.500$		$\beta = -0.100$								

Table 3 Influence of damping on f_{CR}

η/ζ	$\alpha = 0.500$				$\beta = -0.100$			
	.0	.02	.04	.06	.08	.10		
0.8	-1136	-1217	-1298	-1377	-1455	-1532		
1.0	-0760	-1050	-1435	-1570	-1750	-1903		
1.2	-1862	-2676	-2830	-2991	-3165	-3353		

Table 4 (f_1, f_2) at stability limit

η	α	β	PAIR (f_1, f_2) OF CRITICAL VALUE					
			f_1	f_2	f_1	f_2		
1.2	1.0	-0.1	f_1	-1100	-0800	-0700	-0500	-0300
			f_2	-0110	-0776	-1083	-1385	-1696
		-0.5	f_1	-0950	-0850	-0750	-0650	-0550
			f_2	-0050	-0467	-0885	-0885	-1014
1.0	1.0	-0.1	f_1	-0450	-0350	-0250	-0150	-0050
			f_2	-0013	-0302	-0307	-0657	-0959
		-0.5	f_1	-0300	-0200	-0100	-0000	
			f_2	-0215	-0317	-0512	-0962	
0.8	1.0	-0.1	f_1	-0800	-0500	-0400	-0300	-0200
			f_2	-0084	-0039	-0024	-0214	-0326
		-0.5	f_1	-0500	-0400	-0300	-0200	-0100
			f_2	-0152	-0202	-0102	-0033	-0093

$$F(T) = f_1 \sin t + f_2 \sin 1.2t \quad x_0 = 0.002, \dot{x}_0 = 0.$$

CASE 2: $F(t) = f_1 \sin t + f_2 \sin 1.2t$. The pair (f_1, f_2) of stability limit is tabulated in Table 4. Despite that the result of f_2 being considerably small for $\eta = 0.8$ and of f_2 increasing rapidly with decreased f_1 for $\eta > 1.0$ can be foreseen, Table 4 clarifies the tendency of its variation.

CASE 3: $F(t) = \text{random excitation}$. Setting as $\omega_U = 3.0$ and $\omega_L = 1.0$ and

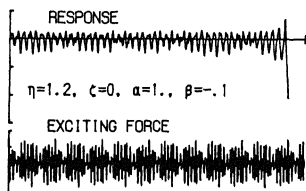


Fig.2 Examples of instability under random excitation

Table 5 S_p, F_m for specific random excitation

η	α	$\beta = -0.1$			$\beta = -0.3$			$\beta = -0.5$		
		f_{CR}	$\sqrt{S_p}$	F_m	f_{CR}	$\sqrt{S_p}$	F_m	f_{CR}	$\sqrt{S_p}$	F_m
1.2	1.0	-1132	.11122	.4205	-1018	.10469	.3958	-1000	.09920	.3751
	0.5	-1962	.20293	.7872	-1590	.17349	.6560	-1388	.15605	.5899
	0.1	-3955	.55892	2.105	-3155	.36271	1.371	-2575	.29044	1.098
1.0	1.0	-0460	.10653	.4028	-0400	.10159	.3841	-0345	.09711	.3671
	0.5	-0760	.19955	.7544	-0572	.16622	.6284	-0493	.14625	.5530
	0.1	-1574	.42535	1.608	-1090	.28622	1.082	-0902	.22812	.8624
0.8	1.0	-0642	.03536	.1338	-0588	.03225	.1219	-0548	.03536	.1337
	0.5	-1136	.04483	.1896	-0912	.05020	.1897	-0786	.04418	.1689
	0.1	-2123	.12336	.4884	-1280	.07382	.2182	-1000	.05840	.2208

$x_0 = 0.002, \dot{x}_0 = 0, \zeta = 0$. Random wave: $\omega_U = 3, \omega_L = 1$, divided into 10 intervals

assuming that power spectrum density between ω_l and ω_u is constant, random excitation was generated and stability critical spectrum density S_p and maximum intensity of excitation F_m were calculated.

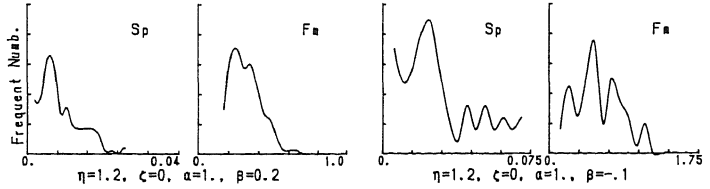


Fig.3 Frequent diagram of S_p and F_m

Fig.2 is an example of dynamic instability under random excitation. S_p and F_m for several η, α , and β with one of random excitation are tabulated in Table 5 from which effects of η, α and β on S_p and F_m can be examined. It seems that inclination of variation of f_{cr} , square root of S_p and F_m with respect to system parameters is quite similar with each other. Fig.3 shows the frequent diagram of S_p and F_m of various random excitation with fixed structural parameters, and correlations between S_p and F_m are plotted in Fig.4. Fig.3 indicates the insuitability of application of simple distribution density function. The fact that S_p is not correlative with F_m as shown in Fig.4 points out that one of the most fundamental and necessary researches on dynamic instability with random or earthquake excitation is to find a suitable indicator of intensity of excitation.

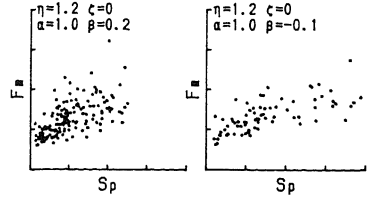


Fig.4 Correlation between S_p and F_m

2. Analytic Prediction of Critical Excitation

As the first step of the research on the prediction of stability limit, the case of sinusoidal excitation will be treated in this paper.

It is easily assumed and confirmed numerically that $\dot{x} = \ddot{x} = 0$ holds at $t=t_1$. It can be concluded, therefore, that the necessary condition for occurrence of dynamic instabilities just like those shown in Fig.1 is $\alpha^2 - 3\beta \geq 0$. If x_1 ($\equiv x|t=t_1$) satisfies, moreover, the condition $dF(t_1)/dx_1 = 1 + 2\alpha x_1 + 3\beta x_1^2 < 0$, successive response is unstable. Therefore, when x_1 satisfies

$$(i) x_{12} < x_1 < x_{11} \text{ for } \beta > 0, \quad (ii) x_1 < x_{12}, x_{11} < x_1 \text{ for } \beta < 0 \quad \dots(6)$$

response is unstable. In case of (i) displacement of the system snaps through to more larger dynamically stable position (there exists limit in displacement) and in case of (ii) displacement increases rapidly to infinity after t_1 . x_{11} and x_{12} represent x_1 relevant to extremum of $F(t_1)$.

Steady state solution of eq.(5) Solution of asymptotic expansion and averaging provides(Ref.5)

$$x(t) = \Phi_1 \sin \xi + \Phi_2 \sin 2\xi + \Phi_3 \sin 3\xi, \quad \xi = \eta t + \theta \quad \dots (7)$$

where $\Phi_1 \sim \Phi_3$ are functions of α, β, f_0 and an amplitude parameter A which is determined by the following equation.

$$(3\beta/4 - 5\alpha^2/6)A^3 + (1 + \alpha f_0/3 - \eta^2)A - f_0 = 0 \quad \dots (8)$$

Eq.(7) with eq.(8) does not present instability phenomena like those in Fig.1. The well known jump phenomenon presented by eq.(8) is different than that discussed here. This solution, therefore, is of no use to obtain f_{cr} . The method discussed by Leipholz(Ref.6) deduces the same jump critical circular frequency of excitation and is not applicable to our problem.

Poincaré map Setting as $\zeta = 0, t = 2n\pi + t_0$ and $t_0 = 0.2, (x_n, \dot{x}_n)$ is numerically calculated and plotted as Figs.5. These figures show continuous

rotation of points plotted rather than staying at one position and denies feasibility of eq.(3). Figs.5, however, seem to suggest that the period of rotation is relevant to f_0 .

Poincaré map-II Plots of (x_n, x_{n+1}) are depicted in Figs.6 in order to examine recurrent character of x_n . It becomes evident from Figs.6 that transfer matrix H which satisfies the following equation

$$[x_{n+1}, \dot{x}_{n+1}]^t = H [x_n, \dot{x}_n]^t$$

is dependent on n and that deterministic expression of H can not be obtained. For f_0 in proximity of f_{cr} , plotted data shape into a triangle as a whole (Fig.6-b). If such a parameter that is relevant to shifting from Fig.6-a to Fig.6-b could be found, f_{cr} would be determined.

Poincaré map-III In order to make clear the influence of beat, that is, super or sub harmonic resonances, the point $[(x_{n+1} - x_n), (x_{n+2} - x_{n+1})]$ is plotted in Fig.7. If all points plotted one by one stay always in the first or third quadrant in Fig.7, response is in dynamic instability. But, Fig.7 denies the existence of such a state. If abscissa and coordinate in Fig.7 are represented as X and Y , respectively, some data seem to be on the line of $Y = -X + const.$ when f_0 is in proximity of f_{cr} (Fig.7-b). Taking lines of $Y = -X$ and $Y = X$ as new abscissa \bar{X} and coordinate \bar{Y} , respectively, and representing the outline curve of data plotted in the third quadrant as follows,

$$\bar{Y} = A \bar{X}^2 + B \bar{X} + C \quad \dots (9)$$

coefficient A will be used as a indicator of stability limit. If A approaches to zero, relevant f_0 is regarded as f_{cr} . An example is shown in Fig.8.

Fourier analysis of $x(t)$ in stability region Some prevailing circular frequencies in stability region included in $x(t)$ with f_{cr} are tabulated in Table 6. This table indicates that $x(t)(t < t_1)$ can be represented as

$$x = D_0 + D_1 \sin t + D_2 \{ \sin, \cos \} (at) + D_3 \{ \sin, \cos \} \{ (1-a)t \} + \dots$$

and a seems to take on the value as

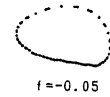
$$\epsilon, 2\epsilon, 1 + \epsilon, 1 - \epsilon, 1 + 2\epsilon, 1 - 2\epsilon, 2, \dots$$

where ϵ is a basic circular frequency parameter. ϵ can be easily found from Poincaré map as inverse of rotation number. This results may infer that dynamic instability in transient region, which behaves as snap through in static instability, is just like chaotic instability which is caused by a lot of bifurcation path.

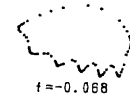
Rough estimation of f_{cr} Setting as $\zeta = 0$, the following equation is deduced from eq.(5).

$$\left[\frac{\eta^2}{2} \dot{x}^2 + \frac{1}{2} x^2 + \frac{\alpha}{3} x^3 + \frac{\beta}{4} x^4 \right]_0^{t_1} = f_{cr} \int_0^{t_1} x \sin t dt \quad \dots (10)$$

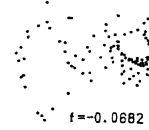
t_1 : time at which $x(t)$ breaks out to instability path



$f = -0.05$



$f = -0.068$



$f = -0.0682$

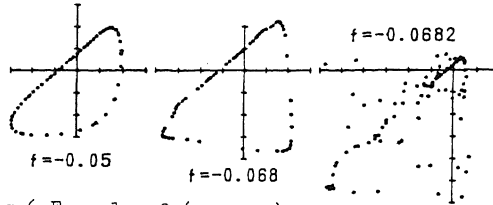
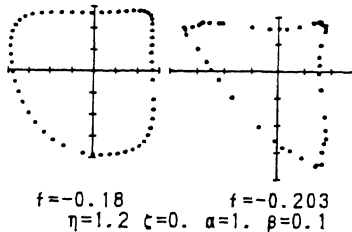


Fig.6 Example of (x_n, x_{n+1}) plot

Fig.5 Example of Poincaré map



$f = -0.18$ $f = -0.203$
 $\eta = 1.2$ $\zeta = 0$ $\alpha = 1$ $\beta = 0.1$

Fig.7 Example of Poincaré map-III

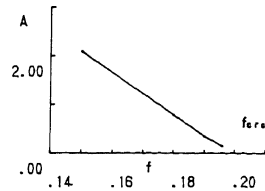


Fig.8 Estimation of f_{cr}

Many numerical examinations indicate that

$$\ddot{x}_1 = \dot{x}_1 = 0, \quad x_1 \equiv x(t_1) \quad \dots\dots (11)$$

Thence,

$$x_1 + \alpha x_1^2 + \beta x_1^3 = f_{CR} \sin t_1 \quad \dots\dots (12)$$

In order to calculate the work done by excitation respondent wave shape should be predetermined. Referring to the results of Fourier analysis, $x(t)$ is set as

$$x(t) = D_0 + D_1 \sin t + D_2(\cos at + \cos bt) + D_3(\sin at \pm \sin bt) \quad \dots(13,14)$$

+ side implies eq.(13) and - side is eq.(14) in this expression. If a and b are previously given, unknowns of $D_0 \sim D_3$, f_0 and t_1 are calculated from these four equations and two initial conditions. These unknowns, however, can not be obtained directly because of nonlinearity of eqs.(10) and (12). In the calculation of x_1 from eq.(12) the condition of eq.(6) is taken into account.

Many numerical examinations lead to that assumption of $\sin t_1 = 1$ seems to be valid.

Results of this examination will be summarized as follows.

(1) Case of $x_0 = 0$, $\dot{x}_0 = f_0(1-\eta^2)$ (if $\eta=1$, $\dot{x}_0=-f_0/2$)

When we set as $a + b = 1$ (applicable to $\eta \geq 1$.), f_{CR} solved by using eq.(14) differs maximum 20% from accurate one given in section 1. In this case, $\sin bt_1$ takes on the value of 0.411581 and that with accurate f_{CR} becomes as 0.414366. That is, the difference between them is very trivial. This implies that f_{CR} is very sensitive to the value of $\sin bt_1$ in this treatment. If the work done by excitation is neglected, f_{CR} of $\eta=1.2$ is in very close agreement with accurate one, but f_{CR} with $\eta \rightarrow 1.0$ leaves from that. If eq.(13) is used, $\sin bt_1$ can not be successfully determined. But, if $\sin bt_1$ is set previously as 0.45 in this case (thence, all equations concerned are not simultaneously satisfied), f_{CR} obtained shows very good agreement with accurate one. And, moreover, f_{CR} becomes not so sensitive to the change of a and b . The case of $a-b=1$ in eq.(14) is included in the case of $a+b=1$ in eq.(13).

(2) Case of $x_0 = \text{const.}$, $\dot{x}_0 = 0$

Usage of eqs.(13) and (14) is unsuitable because $\sin bt_1$ can not be determined for $a \pm b = 1$. If $\sin bt_1$ is predetermined, desirable results can be obtained, though there exists a equation which can not be satisfied.

From the examination just above mentioned it can be concluded that all unknowns included are too sensitive each other and to get desirable results is rather difficult except the treatment of predetermination of $\sin bt_1$. Criterion to predetermine $\sin bt_1$, however, is not definite. But, since this procedure is very simple and can be executed with small personal computer, this will be very practical provided $\sin bt_1$ is predetermined through a few numerical examples.

Table 6 Fourier analysis of $x(t)$ in stability region with f_{CR}

η	α	β	Circular Frequencies of Prevailing Terms					
			1	2	3	4	5	6
0.8	1.0	-0.1	1.000	1.133	0.133	2.000	0.867	1.2666
		-0.5	1.000	1.133	2.000	0.133	0.867	1.2750
	0.5	-0.1	1.000	1.133	2.000	0.133	0.867	1.2666
		-0.1	1.000	1.125	0.875	2.000	0.125	1.2416
1.0	1.0	-0.1	0.8917	1.000	0.7833	1.0883	1.1083	0.8750
		-0.5	0.8917	1.000	0.7833	1.0883	1.1083	0.8833
	0.5	-0.1	0.8833	1.000	0.7583	0.1167	0.6417	1.1167
		-0.1	0.8833	1.000	0.7667	1.1167	0.1167	0.8500
1.2	1.0	-0.1	1.000	0.7167	0.2833	0.4167	0.5833	
		-0.5	1.000	0.7167	0.2833	0.4250	0.5750	
	0.5	-0.1	1.000	0.7167	0.2833	0.4250	0.5750	
		-0.1	1.000	0.7000	0.3000	0.4080	0.5820	1.3000

$$x_0 = 0, \quad \dot{x}_0 = f_0/(1 - \eta^2) \quad f(t) = f_{CR} \sin t$$

REFERENCES

- for instance
J.M.T. Thompson: Proc. R. Soc. London, A387, pp.407 - 427, 1983
J.M.T. Thompson: Appl. Math. Modelling, vol.8, pp.157 - 168, 1984
- J.M.T. Thompson and L.N. Virgin: I.J.Nonlinear Mech., vol.21,no.3,
- H. Kunieda: Proc. 2nd Int. Conf. Space Structures, pp.96 - 103, 1975
- H. Kunieda: SHELLS, MEMBRANES AND SPACE FRAMES, vol.1, pp.33 - 40, 1986
- J.J.STOKER: NONLINEAR VIBRATIONS, Int.Pub., 1950
- H.Leipholtz: Stability of elastic systems, Sijthoff&Noordhoff,1980